nature communications

Article

https://doi.org/10.1038/s41467-026-74737-y

Slowing the spread of treatment failure to artemisinin-based combination therapies in Uganda

Received: 19 July 2025

Accepted: 12 June 2026

Published online: 26 June 2026

Check for updates

Tran Dang Nguyen[1,10], Robert J. Zupko[2,10], Melissa D. Conrad[3], Gerald B. Rukundo[4], Carter C. Farinha[1], Victor D. Asua[5], Kien Trung Tran[1], Deborah M. Grace[2], Philip J. Rosenthal[3], Bosco B. Agaba[4,6,7,8], Moses R. Kamya[4,6,9], Jimmy Opigo[4] & Maciej F. Boni[1]

The continuing spread of partially artemisinin-resistant *Plasmodium falciparum* in Africa is a health challenge that requires urgent attention. The World Health Organization has recommended multiple first-line therapies (MFT) as a response strategy. Implementing a response is critical for Uganda where four artemisinin resistance mutations are at local allele frequencies >0.20 and partner-drug efficacy may be at risk. Using a Uganda-calibrated individual-based mathematical model of *P. falciparum* transmission and evolution, we evaluate 53 public-sector deployment strategies for artemisinin-based combination therapies and report projected reductions in drug-resistance associated treatment failure from 2025 to 2031. Changing first-line therapy from artemether-lumefantrine (AL) to artesunate-amodiaquine (ASAQ) is projected to reduce treatment failures by 34.7% to 38.3% (90% range) while a first-line policy change to dihydroartemisinin-piperaquine (DHA-PPQ) is projected to reduce treatment failures by 10.0% to 12.9%. Optimal MFT deployments and cycling approaches balance their treatment distribution to higher ASAQ use and lower DHA-PPQ use, with projected treatment failure reduction at ~36% when compared to status quo AL use. Deployment of the triple therapy artemether-lumefantrine-amodiaquine is projected to reduce treatment failures by ~42% if enacted immediately. Increased adoption of and coverage with ASAQ is projected to play a large near-term role in reducing malaria treatment failure counts in Uganda.

The 2025 World Malaria Report indicates a slowly increasing global annual case burden, with 282 million malaria episodes and 610,000 malaria deaths estimated for 2024[1]. Across multiple malaria management challenges, one clear and present concern is the spread of artemisinin partial resistance (ART-R) in *Plasmodium falciparum* in Africa. These resistant *P. falciparum* genotypes carry mutations in the *pfkelch13* gene. A total of six validated or candidate mutations—i.e., mutations that are associated with longer parasite clearance times and reduced artemisinin susceptibility in vitro[2]—have been identified across eight countries in east and central Africa[3–5]. This presents a clear

[1]Institute for Genomics and Evolutionary Medicine, Department of Biology, Temple University, Philadelphia, PA, USA. [2]Center for Infectious Disease Dynamics, Department of Biology, Pennsylvania State University, University Park, PA, USA. [3]Department of Medicine, University of California San Francisco, San Francisco, CA, USA. [4]National Malaria Elimination Division, Kampala, Uganda. [5]Institute of Tropical Medicine, University of Tübingen, Tübingen, Germany. [6]Infectious Diseases Research Collaboration, Kampala, Uganda. [7]The Medical Research Council Unit, Banjul, The Gambia. [8]Department of Medical Laboratory Sciences, Faculty of Medicine, Mbarara University of Science and Technology, Mbarara, Uganda. [9]Department of Medicine, Makerere University, Kampala, Uganda. [10]These authors contributed equally: Tran Dang Nguyen, Robert J. Zupko. e-mail: mboni@temple.edu

urgency to respond to and prepare for the further spread of ART-R across the continent[6–8]. Global guidelines for the response are being formulated[9,10] and some national-level response planning is underway[11]. Custom response and preparation strategies will need to be developed as usage of artemisinin-based combination therapies (ACTs), artemisinin and partner-drug resistance landscapes, health systems, and malaria transmission levels differ across countries.

One approach to slowing *pfkelch13* evolution and partner-drug resistance evolution will involve diversification of the partner drugs contained in ACTs[9,12]. The three primary ACTs deployed in this diversification will probably be artemether-lumefantrine (AL), artesunate-amodiaquine (ASAQ), and dihydroartemisinin-piperaquine (DHA-PPQ). AL is the most widely used ACT, and if resistance response efforts are implemented, AL will have its usage rate reduced in many settings[13]; the rationale behind this is that 20 years of consistent AL use has likely led to reduced levels of *P. falciparum* sensitivity to the partner drug lumefantrine[14,15]. Low AL efficacy has been reported in Uganda[16], Angola[1], and Burkina Faso[17]. A fourth ACT that is being considered for increased procurement and accessibility is artesunate-pyronaridine (ASPY)[18,19], which has been shown in therapeutic efficacy studies to have high efficacy in Africa[20–22]. At the moment, the future manufacturing and procurement capacity of ASPY is uncertain. AL and ASAQ are inexpensive and easily procurable, while the costs of ASPY and DHA-PPQ are higher.

Among epidemiological settings in Africa where the spread of kelch variants (falciparum parasites that carry validated/candidate partially artemisinin-resistant *pfkelch13* mutations) has been documented, Uganda's situation is arguably the most dire, with five kelch variants circulating at allele frequencies >0.20 in some districts[23]. Uganda also falls into a group of high-transmission countries where high case numbers and a low detection rate of new infections make many aspects of malaria control challenging. Nevertheless, the Ugandan National Malaria Elimination Division (NMED) began planning artemisinin-resistance response strategies in 2023, with a focus on changing drug policy. Here, we use mathematical modeling to evaluate the first candidate set of approaches that should be discussed in any African context facing spreading artemisinin resistance, specifically changes to first-line therapy, introduction of ACT cycling regimens, deployment of multiple first-line therapies (MFT), and deployment of triple artemisinin-combination therapies.

Results

We use a Uganda-calibrated individual-based epidemiological model of *P. falciparum* transmission, clinical progression, treatment, and evolution (see "Methods") and calibrate the simulation to a July 1, 2025, nationwide parasite prevalence in 2–10 year-olds ($PfPR_{2-10}$) of 17.5% (90% range: 17.4–17.6%). This calibration produces a nationwide reported incidence of 263 malaria cases per 1000 individuals per year. This corresponds to 12.9 million (90% range: 12.83 M–12.96 M) malaria cases reported to the public sector in 2023, close to the 14.2 million to 16.0 million public-sector clinical cases of malaria officially reported in 2023[24]. Using responses from demographic health surveys, 84% of patients in the model receive AL for uncomplicated falciparum malaria, and the remaining 16% receive one of sulfadoxine-pyrimethamine, chloroquine, artesunate monotherapy, quinine, or amodiaquine[25]. On July 1, 2025, the model introduces a treatment strategy for public-sector drug use, and all results for treatment failure counts, treatment failure percentage, and allele frequencies of *pfkelch13* mutations are presented over a six-year period from July 1, 2025, to July 1, 2031. The model keeps private-sector antimalarial drug use constant at 57% of all treatments during this period, with 41.2% of all malaria cases treated with private-sector AL.

Status quo

The continuation of AL as first-line malaria treatment in Uganda is projected to result in increases in malaria burden and substantial increases in treatment failures over the next 6 years. The projection from our Uganda-calibrated malaria simulation model is that from 2025 to 2031, taking the median across all simulation runs, Uganda will experience an annual average of 32.8 million malaria cases, with an annual average of 9.9 million treatment failures or a monthly average of 820,898 treatment failures; the monthly average over 6 years is used here as our quantity for comparison. This assumes no changes in the amount or effectiveness of malaria control activity, only changes in the levels of circulating drug-resistant genotypes. For the first year of the evaluation period (July 1, 2025–July 1, 2026) the model projects a median of 31.2 million malaria cases, with 26.2% treatment failure at the population level across all treatments taken, and in the final year of model evaluation (July 1, 2030–July 1, 2031) the model projects a median 34.5 million malaria cases with 33.1% population-level treatment failure. The monthly treatment failure count (Fig. 1) increases from 684,687 during the first year of implementation to 952,335 over the final year of implementation, corresponding to an annual 6.8% increase in total treatment failures over this period. Note that these treatment failure percentages are reported for the entire population, across public and private markets and across all drugs taken, and they are not comparable to treatment failure rates inferred from therapeutic efficacy studies. The primary reason for the increase in treatment failures over time is the continued use of a single ACT (AL), which is predicted to continue to select for currently circulating kelch variants and any alleles associated with decreased susceptibility to the partner drug lumefantrine.

The rapid increase in ART-R can be seen in the projected sharp rise in the *pfkelch13* allele frequency (Fig. 1). In July 2025, the combined allele frequency of *pfkelch13* alleles 469Y and 675V in Uganda is already estimated to be at a median of 0.91 (90% range: 0.88–0.94), suggesting that a large portion of the parasite population carries one of these two mutations. Note that for 131 out of Uganda's 146 districts, there are no data on *pfkelch13* allele frequencies, and the model's migration mechanism causes these two kelch variants to spread evenly to nearly all districts over the >10 years since their emergence (it is not verifiable if this accurately reflects the true migration process of these variants, and the model does not take into account other variants prevalent in southwestern Uganda[23]). From 2025 to 2031, under the status quo, the combined allele frequency of these two kelch variants is projected to increase to 1.0 (90% range: 1.0–1.0) because they are under strong selection; all population-genetic and evolutionary models would project fixation of these phenotypes under these circumstances (see limitations section of "Discussion").

Switches of first-line therapy to ASAQ or DHA-PPQ

The initial strategies to consider in the face of rising drug resistance are switches to a different first-line ACT, either ASAQ or DHA-PPQ. These two strategies are predicted to have distinct impacts on the projected number of malaria cases, treatment failures, and the spread of ART-R. Both options reflect potential improvements over the status quo, though they come with trade-offs. Under a switch to ASAQ, the total annual average of malaria cases from 2025 to 2031 is projected to be 32.8 million, a 0.3% reduction compared to cases expected under AL. However, ASAQ use results in a lower annual number of treatment failures, estimated at 6.3 million compared to 9.9 million under AL—a 36.4% reduction (Fig. 1). In the first year of the intervention, monthly treatment failures are projected to be 468,881 (90% range: 451,836–482,796), rising to 582,052 (90% range: 568,016–595,055) in the final year (July 2030 to July 2031). For the entire period from 2025 to 2031, the average monthly treatment failures under ASAQ deployment are projected to be 522,456 (90% range: 506,818–535,748). The combined frequency of the 469Y and 675V alleles is estimated to be 0.91 (90% range: 0.88–0.94) in July 2025, and increasing to 0.99 (90% range: 0.99–1.0) by July 2031, as expected under any policy continuing to use ACTs (Fig. 1). While the spread of ART-R is projected to continue

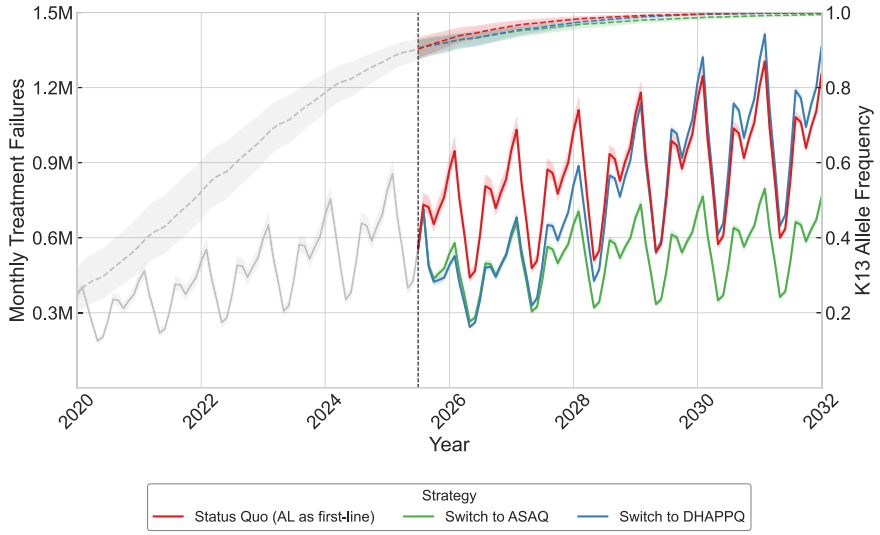

Fig. 1 | Trends in malaria treatment failures and *pfkelch13* allele frequency (2020–2032) under the status quo strategy in Uganda of continued artemether-lumefantrine use (red), a switch to artesunate-amodiaquine (green), and a switch to dihydroartemisinin-piperaquine (blue). Gray lines show the model burn-in and calibration prior to July 2025. Solid lines show monthly treatment failure counts (left axis) while dashed lines show the combined *pfkelch13* allele frequency (sum of frequencies for the 469Y and 675V alleles), which is estimated to be near 0.90 in July 2025. The monthly treatment failure count includes all projected treatment failures for all antimalarials used in the general population. Lines show medians while shaded regions denote the 90% ranges across simulation outcomes ($N = 32$).

under ASAQ deployment, treatment failures will be less common, as the partner-drug resistance landscape will be favorable to amodiaquine treatment even in the presence of *pfkelch13* mutations. This suggests that switching to ASAQ should provide a short- or medium-term solution for mitigating resistance, though it is unlikely to slow the progression of ART-R alleles. ASAQ public-sector deployment, with continued AL use in the private sector, is not projected to drive the evolution of amodiaquine resistance (Fig. 2).

In contrast, switching to DHA-PPQ as first-line therapy results in a lower overall malaria burden (due to the longer half-life of PPQ), but with a substantial additional risk of treatment failure increases. From 2025 to 2031, the annual number of malaria cases under DHA-PPQ is projected to be 31.5 million, representing a reduction of 3.9% compared to AL. However, the total treatment failures are projected to be 31.5 million over the same 6-year period. Monthly treatment failures are projected to be 443,319 (90% range: 429,965–457,492) in year one of the intervention and to rise substantially to 1,036,535 (90% range: 1,021,732–1,046,013) by 2030–2031. For the 2025 to 2031 period, the average monthly treatment failure count for DHA-PPQ deployment is 728,884 (90% range: 715,408–738,795), showing a moderate decrease (11.2% reduction) when compared to status quo AL use. Kelch variants are again projected to reach fixation by 2031 (Fig. 1). Although DHA-PPQ may initially reduce malaria cases and prevalence more effectively than ASAQ or AL, the projected rapid evolution of piperaquine resistance diminishes the long-term utility of DHA-PPQ. It is important to state that, as in our previous analysis for Rwanda[11], the piperaquine-resistant genotypes in our model are parameterized via known PPQ-resistant phenotypes in SE Asia, where DHA-PPQ failure rates reached 58%[26]. It is not known if these same high-failure PPQ-resistant *P. falciparum* phenotypes will evolve in Africa, so there is substantial uncertainty in these treatment failure projections under DHA-PPQ deployment.

2-year cycling approaches

Switching from the status quo to a 2-year cycling strategy in 2025 is projected to substantially reduce malaria treatment failures for most cycling sequences and choices of ACT. Figure 3 shows a summary of monthly treatment failure counts averaged over the six years from 2025 to 2031 for all twelve possible ways to cycle AL, ASAQ, and DHA-PPQ. A cycling approach like this can use either two or three ACTs. The bottom half of Fig. 3 shows that including all three ACTs in the cycling regimen results in similar outcomes regardless of which therapies are used first, second, and third. When two ACTs are used, the projected number of treatment failures depends strongly on which two therapies are chosen. Note that these cycling policies apply only to the antimalarials prescribed in the public sector (43% of all treatments), while AL continues to be used in the private sector for the period of evaluation. The pace of *pfkelch13* evolution is projected to be similar for all twelve cycling options (Supplementary Fig. 4).

The optimal strategy for a 2-year cycling approach is a two-therapy cycle of ASAQ and DHA-PPQ, with ASAQ deployed first. Under this strategy, the projected average monthly treatment failure count for 2025–2031 is 520,568 (90% range: 508,997–537,678), representing a 36.6% reduction compared to the status quo. The second-best strategy starts with DHA-PPQ and cycles to ASAQ; this yields a monthly treatment failure count of 587,119 (90% range: 577,077–605,825), which is a 28.5% reduction compared to the status quo. Note that in both of these strategies, AL is used in the private market, meaning that at any point in time, the on-the-ground treatment usage is either a well-mixed MFT policy with DHA-PPQ and AL or a well-mixed MFT policy with ASAQ and AL. This is likely one of the reasons that these two approaches are associated with the lowest number of projected treatment failures. Among the two-therapy strategies, regimens incorporating AL first are projected to have the highest monthly treatment failure counts, ranging from 723,369 to 732,470, again largely attributable to the substantial use of AL in the private market, resulting in four out of six years in which AL is used for approximately 84% of treatments.

When all three ACTs are included in the cycling strategy, the projected average monthly treatment failure count falls in a narrow range from 607,906 to 627,094, showing a 24–26% improvement over status quo AL use. However, none of these approaches is able to outperform the optimal cycling strategy of ASAQ first and DHA-PPQ second, which takes advantage of (1) the opposing resistance phenotypes seen at the *pfcrt* and *pfmdr1* loci, which make simultaneous drops in efficacy to amodiaquine and lumefantrine difficult to achieve, and (2)

https://doi.org/10.1038/s41467-026-74737-y

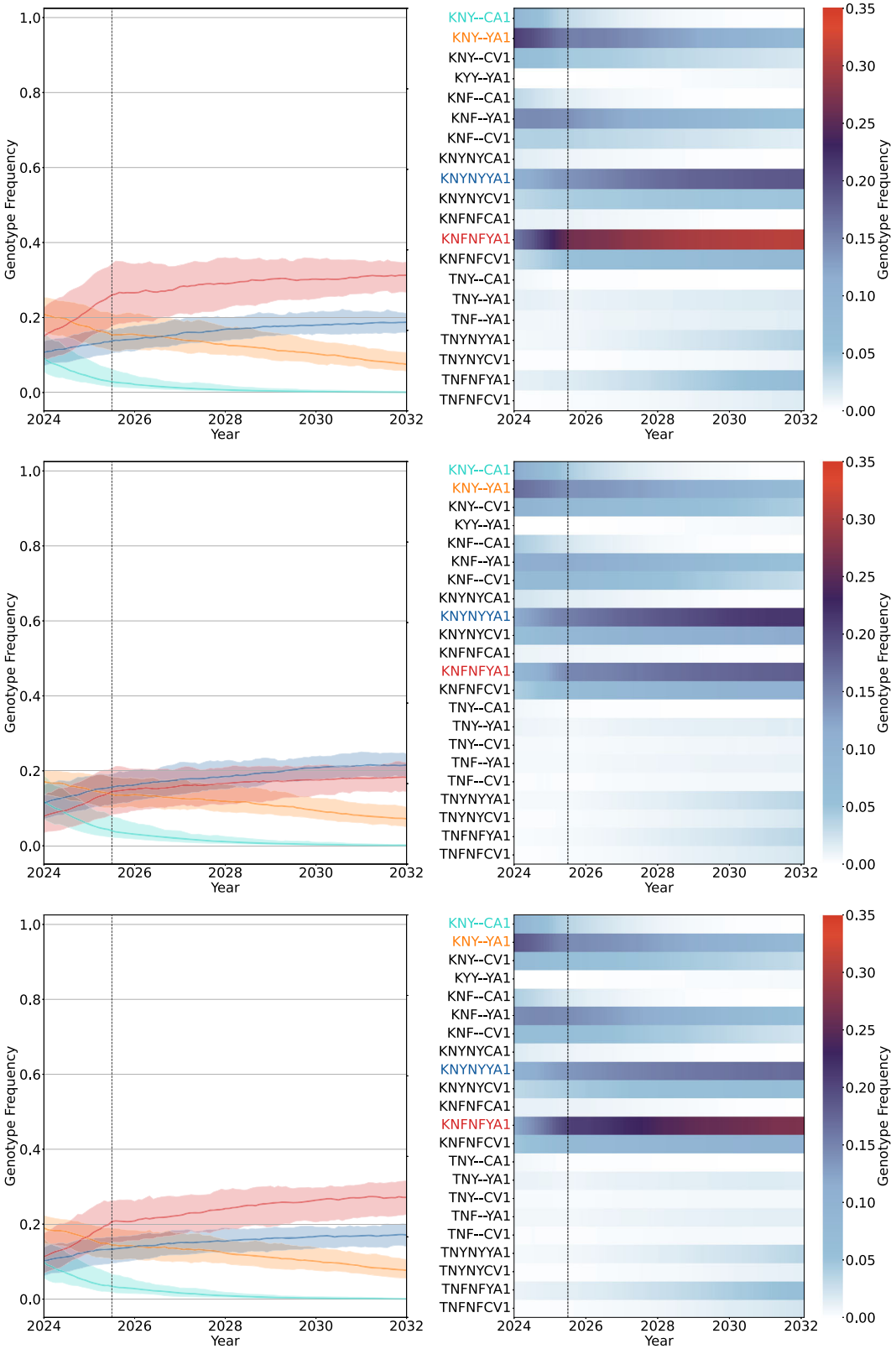

the constancy of AL use in the private market, which allows for a private-public MFT deployment when a non-AL ACT is used in the public sector.

Analyses of individual ACT efficacy show that DHA-PPQ efficacy drops the most quickly among the three ACTs, and that AL efficacy continues to wane even when AL is not deployed in the public sector (Supplementary Fig. 9). The two main reasons for the continuous temporal decrease in AL efficacy are likely (1) persistent use of AL in the private market and (2) model-projected evolution of parasites that are triple-resistant to artemether, lumefantrine, and piperaquine, as can be seen in the right-hand panels of Fig. 4. ASAQ efficacy does not drop below 90% for any cycling strategy or under a strategy that fully switches to first-line ASAQ use for all patients. Again, the usage of AL in the private sector ensures that the evolution of amodiaquine

https://doi.org/10.1038/s41467-026-74737-y

Fig. 2 | Three separate stochastic simulations of genotype evolution under deployment of artesunate-amodiaquine from 2025 to 2032. Left panels show genotype frequencies of three common genotypes (blue, orange, and red) with artemisinin/lumefantrine double-resistance and one common genotype (turquoise) carrying mutations associated with lumefantrine resistance. The red and blue genotypes result in higher treatment failure with artemether-lumefantrine (AL) use due to an additional copy of *pfmdr1* in these parasites, and this higher treatment failure rate allows these two genotypes to outcompete the orange genotype (KNY-YA1). Note that artesunate-amodiaquine (ASAQ) is deployed in the public sector only, and 41.2% of all treatments are private-sector AL use; this results in significant selection pressure from AL during the entire simulation period. Lines show medians, while the shaded area shows 90% range of genotype frequency across all districts of Uganda. Genotype evolution heatmaps for each of the three stochastic simulations are shown in the right-hand column, with each row showing the rise and fall of a particular genotype from 2024 to 2032. Genotype codes (from left to right) are based on the following loci: *pfcrt* K76T, *pfmdr1* N86Y, *pfmdr1* Y184F, *pfmdr1* presence/absence of second copy, *pfkelch13* C469Y, *pfkelch13* A675V, and copy number of plasmepsin genes. Genotypes with early resistance to amodiaquine would show a T in the first position of the genotype code (bottom 7 or 9 rows in each heatmap), but none of these rises to a genotype frequency above 0.12. In 2032, *pfcrt* 76T allele frequencies are 0.15, 0.18, and 0.18 (top to bottom) in the three simulations. All simulated genotypes rising above 0.005 frequency are included in the heatmaps on the right-hand side.

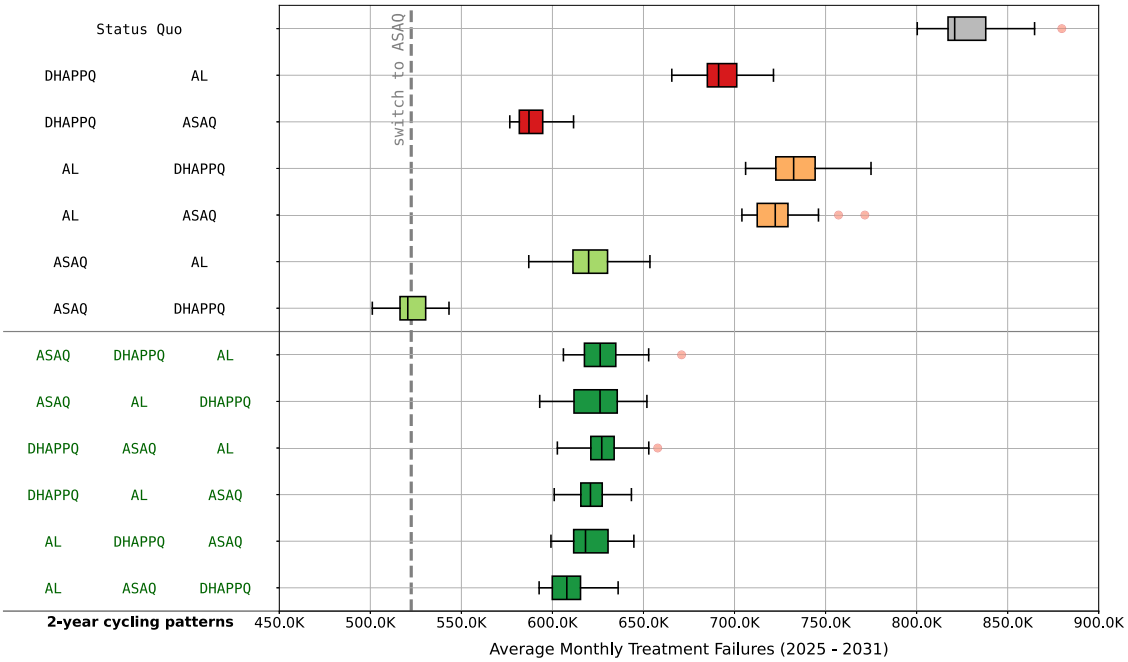

Fig. 3 | Average monthly treatment failures (2025–2031) under different 2-year cycling strategies. These boxplots, summarizing $N = 32$ simulations, illustrate the projected average monthly treatment failures for various 2-year cycling regimens using artemether-lumefantrine (AL), artesunate-amodiaquine (ASAQ), and dihydroartemisinin-piperaquine (DHA-PPQ). The vertical dashed line represents the median monthly treatment failures for a single-drug switch to ASAQ after July 2025. Light green boxplots correspond to two-drug cycles starting with ASAQ, red boxplots represent two-drug cycles initiated with DHA-PPQ, orange boxplots indicate two-drug cycles starting with AL, and dark green boxplots represent three-drug cycling strategies. While three-therapy cycling strategies achieve low treatment failure counts, none of these outperforms a two-therapy cycle of ASAQ followed by DHA-PPQ. Boxplot centers are medians, box bounds show interquartile range, and whiskers show 1.5 times the interquartile range.

resistance faces substantial barriers, as AL has higher efficacy on amodiaquine-resistant parasites.

Finally, as can be seen plainly in Fig. 3, an ASAQ-DHAPPQ 2-year cycling approach is only as good as a straightforward switch to 6 years of ASAQ use. This is because the current set of circulating genotypes in Uganda (*pfcrt* K76, *pfmdr1* N86) will be acted on most efficaciously by ASAQ, per a 2022–2023 therapeutic efficacy study in eastern Uganda showing 100% efficacy of ASAQ[16,27]. The likely reason for this is that genotypes with reduced sensitivity to lumefantrine have been selected for over the past 20 years (in most African contexts), and these genotypes—typically K76 in *pfcrt* and N86 in *pfmdr1*—are most susceptible to ASAQ. This means that most cycling approaches for Uganda can be redesigned around using ASAQ for a longer period first—i.e., a transition period where ASAQ is used as first-line therapy—while operational plans are put into place to transition to a longer-term cycling approach among ACTs and potentially non-ACT therapies if they are made available.

The benefits of cycling approaches with 1-year or 3-year cycles are essentially dependent on how often AL is used during the 6-year period from 2025 to 2031 (Supplementary Figs. 2 and 3). When AL is omitted from the cycling regimen, these approaches also result in a projected average of 540,000 to 550,000 monthly treatment failures, slightly less optimal than the 2-year cycling approach with ASAQ followed by DHA-PPQ.

Multiple first-line therapies

As a standard comparison to drug cycling, we evaluate the deployment of two or three ACTs simultaneously, referred to as MFT[9,28]. Note that in these modeling assessments, it is assumed that patients randomly receive one of several ACTs, and that no specific mechanisms of distribution by age, health facility, or region are used. The standard uniform MFT approach, where each third of the population is treated with one of three ACTs, results in 624,462 monthly treatment failures (90% range: 606,832–644,643), which is a moderate improvement over the status quo (23.9% reduction) but remains a higher failure rate than with the most effective MFT strategies. As in previous analyses[29], the perfectly uniform MFT approach is not always best among all considered strategies, as the current partner-drug landscape and future resistance risk are not equal among the three ACTs.

https://doi.org/10.1038/s41467-026-74737-y

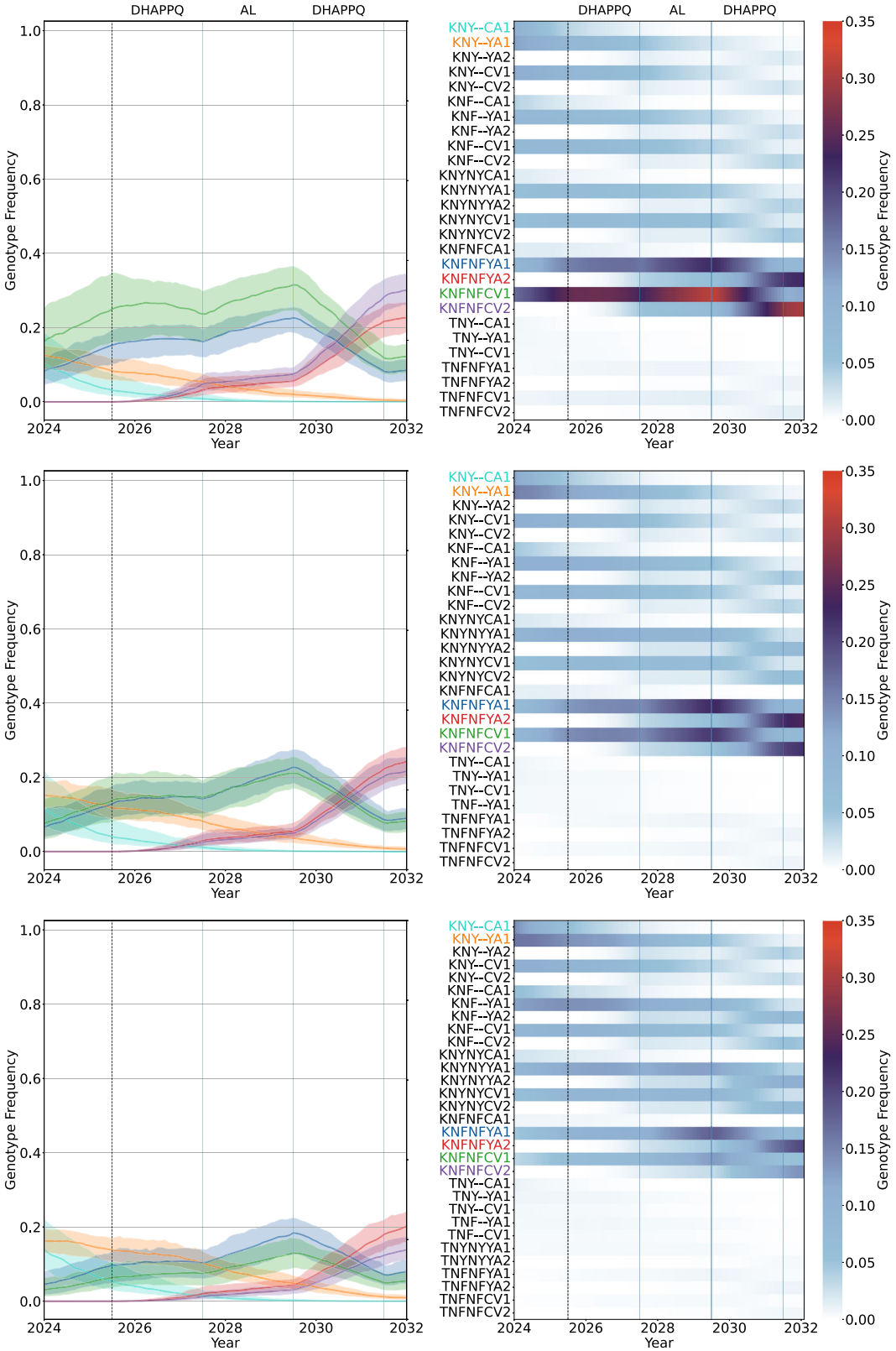

Among MFT options, strategies with lower AL use consistently result in fewer treatment failures compared to those with higher AL use. Figure 5 ranks these strategies by monthly treatment failure count, showing that MFT approaches where 75% of patients receive AL (in red) lead to the highest treatment failure rates, averaging 750,000 per month. While this represents an 8.6% improvement over the status quo, it remains substantially worse than the best-performing MFT strategies. MFT strategies where 25–50% of patients receive AL (in orange) produce monthly treatment failure counts ranging from 600,000 to 700,000—this is still suboptimal when compared to certain treatment strategies (see below) projected to have 520,000 monthly treatment failures. These results emphasize the importance of reducing public-sector AL use while AL is still being widely used in the private sector.

https://doi.org/10.1038/s41467-026-74737-y

Fig. 4 | Three separate stochastic simulations of genotype evolution under a 2-year cycling strategy with dihydroartemisinin-piperaquine (DHA-PPQ) were used first, followed by 2 years of artemether-lumefantrine (AL) use (in both the public and private sectors), and then followed by 2 years of DHA-PPQ use (public sector only). AL is used in the private sector throughout. Left panels show genotype frequencies of six common genotypes: five of these carry a *pfkelch13* mutation, and two of these genotypes (red, purple) carry triple resistance to lumefantrine, piperaquine, and artemisinin. In these simulations, we see that double-resistance to AL (blue, green) continues to be selected for, from 2026 to 2029, whether DHA-PPQ is used in the public sector or not. From mid-2027 to mid-2029, when AL is used in both public and private sectors, double-resistant genotypes to AL are selected for, and the KNFNFYA1 (blue) and KNFNFCV1 (green) genotypes remain at high levels. When DHA-PPQ is deployed for the second time in July 2029, the two triple-resistant genotypes (KNFNFYA2 and KNFNFCV2) are selected quickly because PPQ resistance has a large fitness advantage (high treatment failure rate) over PPQ sensitivity. Lines show medians, while shaded areas in the left panels show 90% range of genotype frequency across all districts of Uganda. Genotype evolution heatmaps for each of the three stochastic simulations are shown in the right-hand column, with each row showing the rise and fall of a particular genotype from 2024 to 2032. Genotype codes (from left to right) are based on the following loci: *pfcrt* K76T, *pfmdr1* N86Y, *pfmdr1* Y184F, *pfmdr1* presence/absence of second copy, *pfkelch13* C469Y, *pfkelch13* A675V, and copy number of plasmepsin genes. All simulated genotypes rising above 0.005 frequency are included in the heatmaps on the right-hand side.

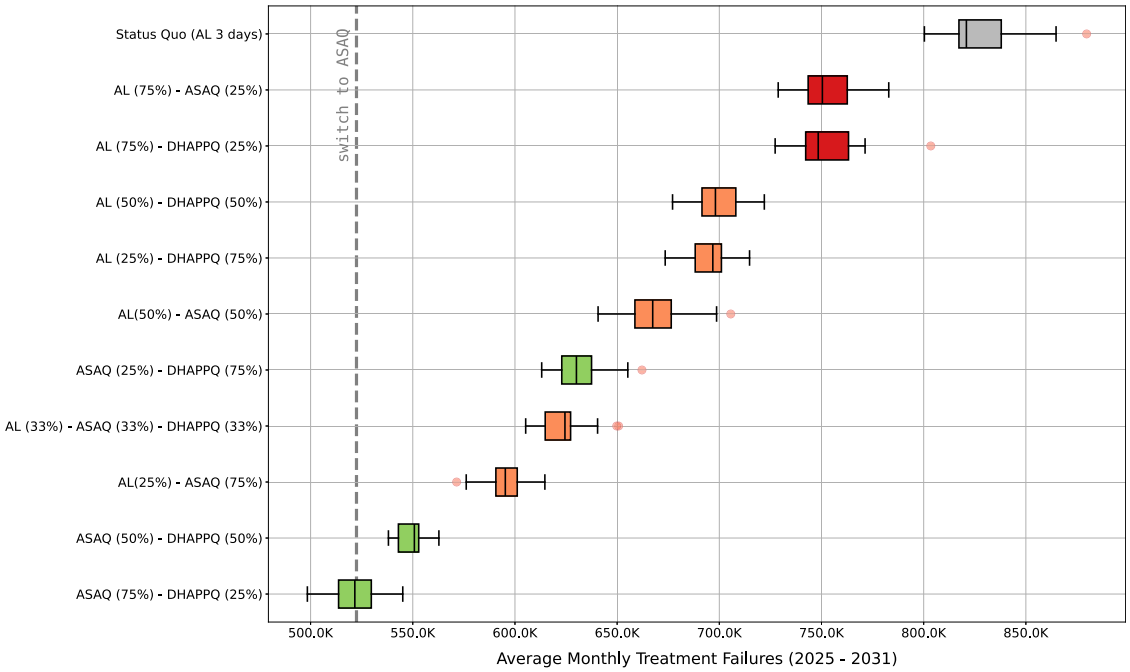

Fig. 5 | Average monthly treatment failures (2025–2031) across different MFT strategies. Each boxplot summarizes $N = 32$ simulation outcomes and shows the average monthly treatment failure count, from 2025 to 2031, under various multiple first-line therapies (MFT) strategies. Strategies differ according to the different proportions of artemether-lumefantrine (AL), artesunate-amodiaquine (ASAQ), and dihydroartemisinin-piperaquine (DHA-PPQ) that are deployed in the public sector. The status quo corresponds to continued use of AL and has the highest median monthly treatment failure count at 820,898. MFT strategies are color-coded based on AL usage: green represents strategies with no AL; orange shows strategies where AL represents 25–50% of treatments; red shows strategies where AL is used for 75% of malaria cases. The vertical dashed grey line represents the median monthly treatment failures observed for a first-line switch to ASAQ. The MFT strategy with the lowest average monthly treatment failures is ASAQ (75%)—DHA-PPQ (25%), achieving a median monthly treatment failure count of 521,649, a 36.5% reduction compared to the status quo. Boxplot centers are medians, box bounds show interquartile range (IQR), and whiskers show 1.5 IQR.

The optimal MFT choice in Fig. 5 combines ASAQ (75% use in the population) and DHA-PPQ (25% use), taking advantage of the beneficial partner-drug resistance landscape to amodiaquine and a relatively low level of PPQ use to weaken the selective pressure on piperaquine-resistance evolution. This approach is projected to generate an average of 521,649 treatment failures (90% range: 505,669–538,608) per month, corresponding to a 36.5% reduction compared to the status quo. Thus, the best MFT strategy has a nearly identical treatment failure outcome as (1) the best cycling strategy and (2) a switch to first-line ASAQ use, again underscoring the utility of using ASAQ as a transitional therapy for the second half of the 2020s. ASAQ efficacy is projected to stay >90% for all evaluated MFT strategies, as AL use in the private sector counteracts potential AQ resistance evolution (Supplementary Fig. 9).

Options for triple ACT deployment

Finally, the largest reduction in near-term and medium-term treatment failure counts is projected to result from deployment of the triple therapy artemether-lumefantrine-amodiaquine (ALAQ). This is consistent with projections from a past multi-model comparison[30], our analysis of ALAQ deployment in Rwanda[11], and evaluation of ALAQ deployment with a new, more complex 25-locus individual-based model of *P. falciparum* evolution[31]. Switching to a triple artemisinin-based combination therapy (TACT) offers a promising avenue for reducing malaria treatment failures and slowing the spread of resistance. However, the timing of the transition—whether immediate or delayed—affects this strategy's efficacy. While immediate implementation of ALAQ is the most effective strategy[30], the time required for regulatory approval, manufacturing, and establishment of supply chains necessitates interim approaches. Here, we simulate a four-year delay before ALAQ is approved as a first-line therapy, with alternate regimens used during the interim period.

An immediate switch to ALAQ yields the fewest treatment failures, with a monthly average of 477,929 (90% range: 463,464–499,508), which is 41.8% lower than the status quo forecast of 820,898 (Fig. 6). If ALAQ is not available until July 2029, the best interim approach is to

https://doi.org/10.1038/s41467-026-74737-y

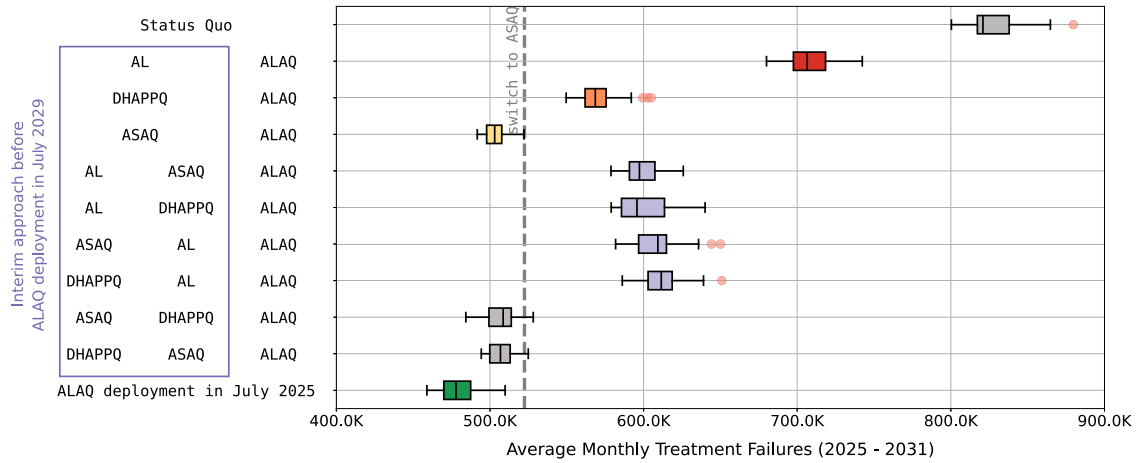

Fig. 6 | Average monthly treatment failures (2025–2031) under different deployments of the triple artemisinin combination therapy artemether-lumefantrine-amodiaquine (ALAQ). Boxplots summarize $N = 32$ simulation outcomes and show the average monthly treatment failure counts for the period 2025–2031 for various ALAQ deployment scenarios. The vertical dashed grey line represents the median monthly treatment failures observed when artesunate-amodiaquine (ASAQ) is used as first-line therapy after July 2025. If ALAQ is not available until July 2029, the best interim approach is to switch to ASAQ for four years or implement a 2-year cycle of ASAQ and dihydroartemisinin-piperaquine (DHA-PPQ) before transitioning to ALAQ. These strategies effectively balance resistance management and treatment efficacy, with projected monthly treatment failures averaging ranging from 503,000 to 508,000. These represent substantial reductions in treatment failure counts compared to the status quo. In contrast, continuing artemether-lumefantrine (AL) use for four years before introducing ALAQ results in the worst outcomes, with monthly treatment failures reaching 706,494 (90% range: 687,993–736,851). This comparison highlights the effectiveness of an immediate switch to ALAQ and underscores the advantage of minimizing AL use as an interim strategy when ALAQ deployment is delayed. Boxplot centers are medians, box bounds show interquartile range (IQR), and whiskers show 1.5 IQR.

switch to ASAQ for four years or implement a 2-year cycle of ASAQ followed by DHA-PPQ before transitioning to ALAQ. These strategies effectively balance resistance management and treatment efficacy, with projected monthly treatment failures averaging 503,067 (90% range: 493,290–519,556) under the 4-year ASAQ approach (a 38.7% reduction compared to the status quo) and around 506,000–508,000 when cycling ASAQ and DHA-PPQ.

In contrast, continuing AL use for four years before introducing ALAQ is the worst option among the evaluated strategies, with monthly treatment failures reaching 706,494 (90% range: 687,993–736,851), still a 13.9% reduction compared to no TACT switch (Fig. 7, red line). While all TACT deployment options outperform the status quo, strategies that include 2-year cycling with AL (lavender box plots in Fig. 6) before switching to ALAQ lead to higher treatment failure counts and delay the full benefits of ALAQ, reinforcing the importance of minimizing AL use in transition plans.

Effects of artemisinin monotherapy use

Artemisinin monotherapy use has been discouraged globally by the WHO since the adoption two decades ago of guidelines recommending ACTs for first-line use[32–36]. Nevertheless, parenteral artesunate monotherapy use is common in many private-sector health care settings[37–39], and there is no way to independently validate the current survey-based[40] estimate of 4.8% of uncomplicated malaria cases being treated with an artemisinin-based monotherapy. As such, it is possible that selection pressure for the recent increase in *pfkelch13* mutations in East Africa has come partially from AL use and partially from artemisinin monotherapy use. We investigated scenarios of earlier artesunate monotherapy introduction and a range of usage rates from 0 to 20%, which suggests that increased usage of parenteral artesunate does have the potential to accelerate the evolution of *pfkelch13* mutation by a year or two (Supplementary Fig. 10).

Discussion

As of 2023–2024, among all countries in Africa, Uganda had the highest allele frequencies of *pfkelch13* mutations confirmed to be associated with artemisinin partial resistance. Five unique kelch variants had spread to at least 15 districts in Uganda by late 2022. There has been some evidence of ~10% treatment failure rates to AL over the past 10 years[41,42] and recent evidence of 18% PCR-corrected AL treatment failure in two districts in Uganda[16,27,43]; surprisingly, at each of these two sites, the allele frequencies of *pfkelch13* mutations that mediate artemisinin partial resistance were low. The Ugandan NMED has recognized the urgency of this situation and, in 2023, began putting plans into place to mitigate the effects of spreading partial artemisinin resistance. The majority of strategies designed to counter the spread of resistance focus on altering the deployment of first-line antimalarial therapies in order to maximize current treatment efficacy against circulating *P. falciparum* genotypes and slow down the spread of mutations associated with partner-drug resistance. This report describes a first-phase evaluation of common treatment strategies available to the Uganda NMED in the second half of this decade.

Our mathematical modeling analysis projects that, over the next 6 years: (1) continued use of AL as first-line therapy will result in an annual ~7% increase in treatment failures; (2) a switch to ASAQ as first-line therapy would reduce treatment failure counts by approximately 36.4%—assuming prompt implementation and high levels of compliance; (3) cycling approaches and MFT approaches that are balanced toward higher ASAQ use and lower DHA-PPQ use will also lead to ~36% reductions in projected treatment failure counts; and (4) immediate deployment of TACT would lower absolute treatment failure counts by ~42%. These standard national-level strategy designs have room for improvement in their adaptation to specific epidemiological contexts, adjustment for regional drug efficacy estimates, and enhancement by public health communication measures. If ASAQ deployment becomes a major part of Uganda's ART-R response in the 2020s, continued routine surveillance of AQ-resistance will be essential.

The size of Uganda's private antimalarial market has a substantial influence on the optimal choice of ACT deployment in the public sector. We assume in this analysis that private-sector drug purchases cannot be influenced in the near-term by national-level treatment guideline changes, meaning that under all treatment scenarios, AL will be used for 41% of all malaria cases, and a non-ACT treatment will be used for another 16% of cases treated through

https://doi.org/10.1038/s41467-026-74737-y

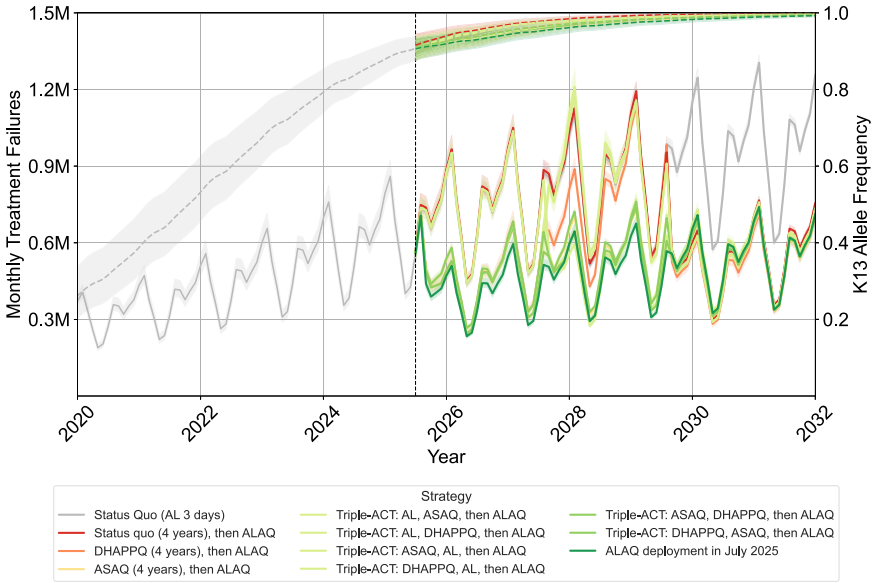

Fig. 7 | Trends in malaria treatment failures and *pfkelch13* allele frequency under different deployment options for the triple artemisinin combination therapy artemether-lumefantrine-amodiaquine (ALAQ), from 2025 to 2032. Gray lines show the model burn-in and calibration prior to July 2025. Solid lines show monthly treatment failure counts (left axis) while dashed lines show the combined *pfkelch13* allele frequency (sum of frequencies for the 469Y and 675V alleles). The monthly treatment failure count includes all projected treatment failures for all antimalarials used in the general population. Lines show medians while shaded regions denote the 90% ranges across simulation outcomes ($N = 32$). Dark green line corresponds to immediate deployment of ALAQ, which achieves the best outcomes by keeping the average monthly treatment failure count below 500,000 and somewhat slowing the fixation of kelch mutations. The lighter green lines show 2-year cycling approaches using artesunate-amodiaquine (ASAQ) and dihydroartemisinin-piperaquine (DHA-PPQ) before switching to ALAQ. The orange line (DHA-PPQ), yellow line (ASAQ), and red line (AL) represent scenarios where a single artemisinin-based combination therapy is used for four years before transitioning to ALAQ.

private pharmacies or dispensaries. Our strategy comparisons indicate that we can take advantage of these fixed preferences in the private sector and utilize ASAQ or DHA-PPQ in the public sector to achieve a locally mixed deployment of therapies by combining private-sector AL and public-sector ASAQ or DHA-PPQ (note that this approach would change if private-market preferences changed). The assumption is that public clinics/dispensaries and private pharmacies or shops co-exist in the same spaces and that there are no strong local preferences to seek treatment in a private versus a public facility. The modeling outcome is that different public-sector and private-sector treatment regimens will slow the increase in drug-resistance-associated treatment failures because local use of two (or three) ACTs ensures that a patient has a 1-in-2 (or 2-in-3) chance of using an ACT whose partner-drug has high efficacy on their particular form of partner-drug resistance. The general conclusion from this dynamic is that optimal strategies for the near-term and medium-term are those that recommend high or even 100% ASAQ use in the public sector. A reasonable and near-optimal long-term approach would be to use ASAQ as a transitional therapy until triple therapies or non-ACT combinations become available.

When considering policy changes in Uganda, there is no guarantee that a geographically uniform national-level policy will be optimal among all available strategy choices, and there is likewise no guarantee that a regionally targeted and context-specific design would have the high compliance and friction-free implementation needed to be as effective as projected in a mathematical model. Nevertheless, locally targeted strategies must be considered, including specific designs for low-prevalence areas amenable to elimination efforts and increases in vector control, neither of which is considered in this analysis. In general, if it is known in some region that either (a) a history of drug use or (b) currently circulating genotypes indicate that certain ACTs are likely to have higher local efficacy than others, a customized region-specific ART-R response strategy should be considered. A second phase of treatment strategy design should evaluate combinations of locally tailored approaches and deployment of novel therapeutics when they are made available.

A key tool for any resistance mitigation effort in the 2020s is the deployment of artesunate-pyronaridine, an ACT that has the advantages of high efficacy[13,30] and no known resistance genotypes and the disadvantages of high price and difficult procurement. Pyronaridine does not appear to readily generate high-grade resistance in vitro. ASPY deployment is an ideal option in an MFT or cycling approach whose aim is to lower the resistance pressure on currently deployed partner drugs and also increase the population-average treatment efficacy of the therapies in use in the population. Additionally, in the coming years, as ganaplacide-lumefantrine[44,45] and single low-dose primaquine[46,47] are being positioned for addition to treatment guidelines for uncomplicated falciparum cases, these novel therapies should have their resistance and transmission effects evaluated via mathematical modeling analyses. Introduction of novel therapies would allow decreased AL use and would relieve the pressure on amodiaquine and piperaquine resistance evolution, both having occurred in the past.

Limitations

The major limitations in this analysis center on (1) our inability to precisely match genotypes to drug-resistance phenotypes[48], and (2) the lack of predictability around which individual mutations will arise first in certain contexts[49]. An area of particular uncertainty is our limited knowledge on the complex evolutionary pathways that lead to piperaquine resistance and which of these pathways is the most likely to occur in African malaria settings. Four mutations in the *pfcrt* gene (T93S, H97Y, F145I, and I218F) rose to high enough frequency in Cambodia that their effects on reduction of DHA-PPQ efficacy could be measured[50], but it is not known which of these or potentially other mutations with in vitro associations with PPQ-resistance[51–54] will be the first to emerge and be selected for in Uganda (or elsewhere in Africa). As stated in our previous analysis on this topic[11], the uncertain future of

piperaquine resistance evolution in Africa is the major risk that needs to be managed as multiple ACTs are deployed. This is not to say that DHA-PPQ should not be deployed as a component of ART-R response in Africa. On the contrary, DHA-PPQ deployment will likely play a critical role in any successful response by increasing near-term treatment efficacy. However, introduction and scale-up of DHA-PPQ should aim for moderate levels of DHA-PPQ usage at a population-level[9], and DHA-PPQ deployment should be accompanied by rapid-turnaround real-time molecular surveillance for known resistance markers[13].

Second, compliance and implementation are persistent challenges for any change in malaria treatment guidelines. Several recent studies have aimed to collect qualitative information on compliance with treatment recommendations, drug stock management, drug distribution choices, and general acceptance of the need to prepare for the coming challenge of drug resistance[55–57]. These studies suggest that acceptability for changes in treatment policies is high and that novel drug management approaches will be feasible; however, the final proof can only come from on-the-ground implementation occurring outside a research context. Adherence to ASAQ use will play an important factor in every strategy; reduced preference for ASAQ due to gastrointestinal intolerance or other symptoms will need to be monitored to determine if planned and realized ASAQ deployment coincide. Antimalarial sales in unregulated outlets will also need to be monitored, as it is known that partial ACT courses, parenteral artesunate monotherapy, and non-ACT treatments can be purchased; these are likely to have detrimental effects on resistance evolution and treatment failure counts.

Third, in modeling analyses, ASAQ use will also have to be assessed alongside the use of amodiaquine in seasonal malaria chemoprophylaxis (SMC) programs, which use a monthly combination of sulfadoxine-pyrimethamine and amodiaquine (SPAQ). Simultaneous use of ASAQ and SPAQ could increase the rate of AQ-resistance evolution. Although SMC has mostly been used in West Africa, it was recently initiated in northeastern Uganda[58], where malaria incidence is relatively seasonal. If SMC is expanded in Uganda, several million children may eventually be covered by the program, potentially receiving between 10 and 20 million courses of SPAQ, several million of which would be administered to parasite-positive children. This means that deployment of first-line ASAQ for symptomatic uncomplicated falciparum malaria in the public sector would entail about 13 million ASAQ treatments in higher-parasitaemia symptomatic cases alongside several million SPAQ treatments for children with lower-parasitaemia asymptomatic infections. There is no simple way to determine the additional evolutionary pressure on amodiaquine resistance evolution generated by SPAQ use; thus, a separate modeling analysis with known SMC distribution data will need to be carried out. This separate analysis will also need to account for the importation of AQ-resistant parasites by newly arriving refugees from South Sudan, where ASAQ is currently first-line therapy[59].

Fourth, data on the 2025 allele frequencies of circulating kelch variants in Uganda have only recently been collected. As ACTs continue to be used in Uganda and across Africa, modeling analyses predict that genotype frequencies of kelch variants will increase in the near term. Our modeling analysis projects that the combined frequency of the *pfkelch13* 469Y and 675V alleles was already 0.91 (90% range: 0.88–0.94) in mid-2025, implying that these slow-clearance phenotypes may already be near fixation in 14 or 15 districts in Uganda. The most recent data from this region (Okitwi et al.[14] and unpublished data) demonstrate summed kelch genotype frequencies nearer 0.50 in many districts, suggesting certain epidemiological or parasite factors limiting the spread of ART-R genotypes. It is not possible at the moment to know how accurate our model projections are on a per-allele or per-genotype basis. The strong selection pressure in our model is based on the high ACT coverage reported in Uganda (>80% in all MIS regions) and the rapid movement and transportation of these parasites around the country. The next iteration of country-level model calibration in Uganda will need to include validation metrics on the strength of selection pressure, fitness constraints of resistance mutations, the pace of evolution, the movement of parasites around the country, and an accounting (if possible) of all genotypes that are potentially being selected.

Finally, the procurement of all ACTs in Africa was put in jeopardy in 2025 by the closing of the United States State Department's President's Malaria Initiative (PMI), which is estimated to leave a gap of approximately half of all ACTs procured in Africa[60]. The sudden loss of PMI programs and resources is projected to increase malaria deaths in Africa by approximately 100,000 if ACT stocks are depleted and new funding mechanisms are not identified[60,61], and this would undoubtedly have a large impact on country programs' ability to prepare for the coming fight against artemisinin resistance. The specific challenge of procuring more types of ACTs, including the more expensive ACTs (DHA-PPQ and ASPY), when financing has disappeared, was not modeled in the present analysis.

As the artemisinin-resistance response moves forward in Africa, continual monitoring and real-time data collection are essential. Therapeutic efficacy studies are a particularly important component of this effort, as this will be the only way to know when increasing *pfkelch13* allele frequencies and high-grade partner-drug resistance combine to drive treatment efficacies to low levels. Crucially, results from therapeutic efficacy studies must be accompanied by genotyping of polymorphisms known or strongly suspected to be associated with clinical drug-resistance[31]. This is especially important for understanding the predictive ability of certain partner-drug resistance alleles on treatment failure. The population-level treatment strategies evaluated in this analysis act by favoring some genotypes over others, and the genotype information contained in therapeutic efficacy studies is the most direct way to know which genotypes are associated with failure and thus which genotypes should be targeted for reduction by a treatment strategy.

Adoption of novel treatment strategies this decade in the African countries where kelch variants are currently circulating will be critical for the rest of the continent as treatment policy decisions are made and as *pfkelch13* alleles arrive in new locations, demanding new mitigation measures. In Uganda, the appropriate response—as projected from this modeling analysis—is to switch to ASAQ as a transition strategy and decide whether to proceed to a rotational approach, triple ACT adoption, or a variant of an MFT strategy. We recommend that this strategy change be instituted soon, as continued use of AL is projected to drive treatment failure counts higher every year. Once this challenge is met, the next step in the drug-resistance mitigation process—in Uganda and in all African countries facing increasing treatment failures—will be to replace at least some ACT use with non-artemisinin-based combination therapies to attempt to reverse *pfkelch13* evolution and to recover recently lost treatment efficacy.

Methods

Ethical approval was not required for this study as no primary data were collected and no personal health information was accessed.

Geography, population, and travel time

As described previously[11,29], a spatial individual-based *Plasmodium falciparum* transmission and evolution model was calibrated to Uganda's geography, population, malaria prevalence, and malaria treatment patterns. Shapefiles (national and subnational boundaries) for Uganda were downloaded from the Humanitarian Data Exchange[62] along with the 2018 Malaria Indicator Survey (MIS) boundaries[25], and converted to the appropriate file type and re-projected as necessary to WGS 84/ UTM zone 36N (WKID 32636). Since the simulation runs in a spatial configuration based on the raster data, misalignments between the subnational boundaries and the MIS boundaries were not

https://doi.org/10.1038/s41467-026-74737-y

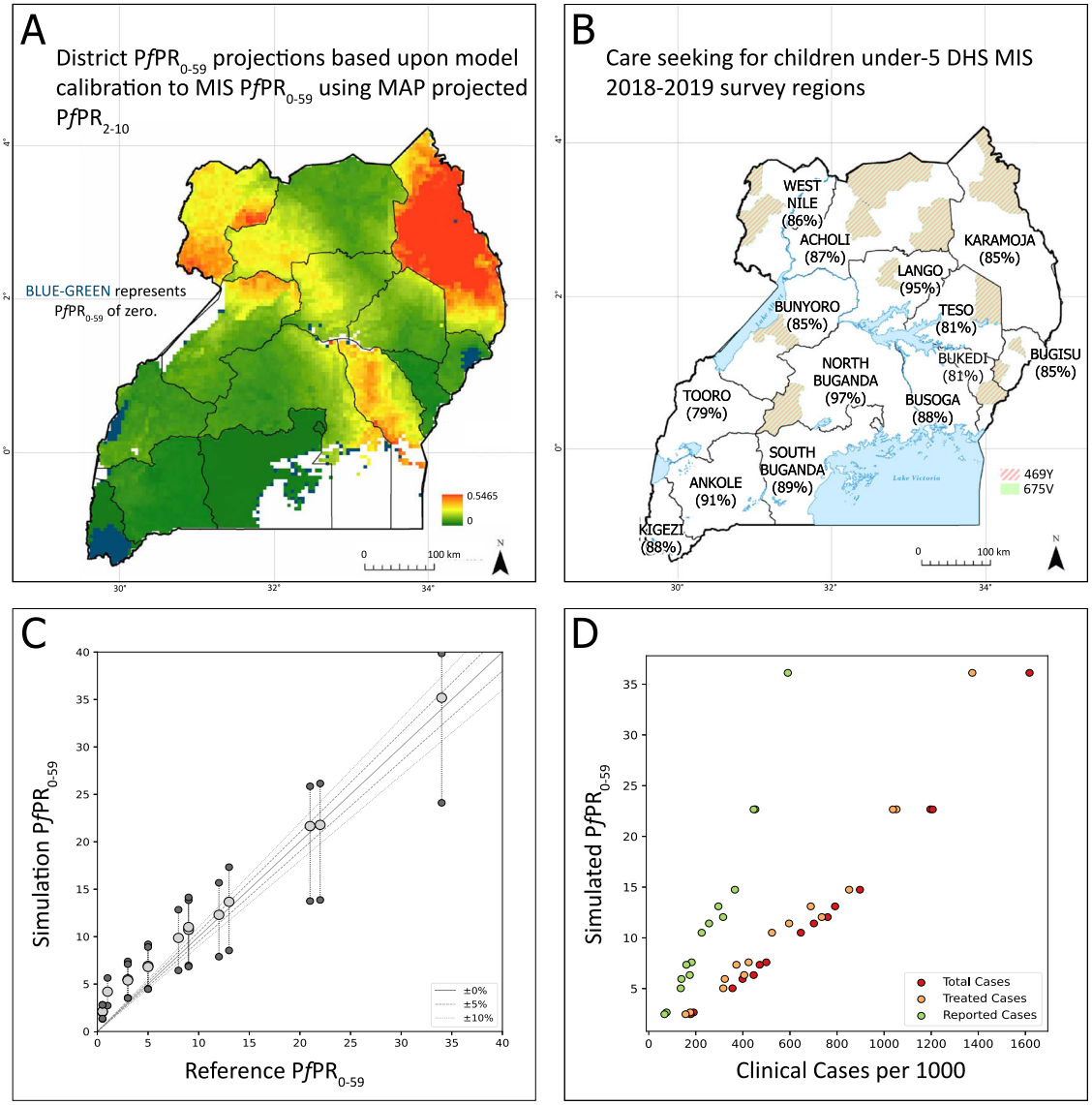

Fig. 8 | Model calibration to malaria prevalence, treatment-seeking rates, and reported incidence. A Final prevalence ($PfPR_{0-59}$) calibration derived from Malaria Atlas Project estimates for $PfPR_{2-10}$ in 2017, and later adjusted to Malaria Indicator Survey (MIS) $PfPR_{0-59}$ values from 2018 to 2019[40]. Map prepared by authors using simulation outputs, MIS 2018 DHS Regions Boundaries[25], and Uganda Boundaries[62]. **B** Treatment coverage for children under five, according to the 2018–2019 MIS. Shaded districts show districts where *pfkelch13* alleles 469Y or 675V have been identified. **C** Comparison of model-simulated prevalence in MIS districts to MIS data. The gray dot shows the annual mean prevalence in 0–5 year-olds, while the dark gray dots at the top and bottom indicate the intra-year upper and lower bounds. **D** By MIS district, the incidence of simulated malaria cases per year (red), the incidence of simulated malaria cases that are treated (yellow), and the incidence of treated cases that are likely to be reported to the public health system (green) based on treatment-seeking choices made between private and public sectors. Incidence is shown as annual cases per 1000 individuals (x-axis) and plotted against the simulated $PfPR_{0-59}$ (y-axis).

addressed, and the subnational boundaries were used as the canonical source when preparing the raster files for the simulation. Individual mortality and population demographic data were based upon the United Nations World Population Prospects reports from 2019.

Following preparation of the shapefiles, raster data were next augmented by acquiring the 2020 population density data from WorldPop[63], which were then re-projected and aggregated to 25 km^2 pixels from 30 arc-second pixels, with rounding up to the nearest whole number. This resulted in a total of 8566 grid points, which were assigned to one of fifteen MIS districts in Uganda based upon the 2018 MIS boundaries[25]. The aggregated data were then clipped to match the regional boundaries defined above. A similar process was used for the travel friction surface, which was acquired from the Malaria Atlas Project's map of travel time in minutes to the nearest city, for the year 2015[64]. The travel friction surface is used to augment a gravity model of travel in sub-Saharan Africa[65], by biasing individuals' travel to the nearest large city as opposed to the largest city in the country[66] (Supplementary Figs. 5–7).

A seasonal transmission function was derived from rainfall data as in previous modeled scenarios[11,29] (Supplementary Fig. 1). Pixel-level malaria prevalence was calibrated according to the treatment-seeking rates in each pixel (as described previously[11]) and is detailed in Supplementary Methods S1.1. Figure 8 shows the model's final calibrated prevalence, treatment seeking, and MIS district-level incidence.

Incidence calibration

We verified that the final $PfPR_{0-59}$ (prevalence in children <60 months of age) was within ±1% (in absolute terms, for 14 of 15 MIS regions) of the estimates from the 2018 MIS. The clinical case counts per 1000 individuals were also checked against the target calibration year of

2020. In the simulation, all clinical cases (i.e., symptomatic episodes of malaria) were logged along with their treatment or lack thereof; not all treated cases of malaria are considered as reported due to private-sector treatment seeking. Based on the 2018–2019 MIS[40], about 44% of treatments were seen at private hospitals or clinics, with another 14% seeking treatment at private shops or pharmacies; an estimated 43% of treatments were seen in the public sector and reported. As such, for the target calibration year of 2023, there were an estimated 34.0 million clinical cases of malaria in the model, with 29.9 million treated, and 12.9 million reported in the public sector. While the model's projection of total reported cases is low compared to the 14.2–16.0 million public sector clinical cases reported in Uganda in 2023[1], the model's prevalence projection is within the margin of error of the MIS district $PfPR_{0-59}$ values from the simulation. The emergence of two *pfkelch13* mutations was calibrated in this fixed prevalence and incidence setting (Supplementary Methods S1.2 and Supplementary Fig. 8). The *pfcrt* K76 and *pfmdr1* N86 alleles are fixed in Uganda; the *pfmdr1* 184F allele has been reported at between 0.20 and 0.30 allele frequency in different districts. These three allele frequencies were fit manually after the *pfkelch13* calibration above. Piperaquine-resistant genotypes are assumed in the model to start at zero frequency in 2025.

Genotype-to-phenotype drug resistance model

As described previously[48,49], we model a 7-locus genotype for all falciparum strains, resulting in 128 genotypes in the model. The loci are *pfcrt* K76T, *pfmdr1* N86Y, *pfmdr1* Y184F, *pfkelch13* C469Y, and *pfkelch13* A675V. Copy number variation (CNV) for the *pfmdr1* and *plasmepsin-2,3* genes are included. Each genotype-therapy combination is mapped to 28-day PCR-corrected efficacy via a previously published 64 × 10 drug-by-genotype (DxG) table. In the current analysis, the *pfkelch13* loci 469 and 675 have independent but phenotypically identical effects[67]. According to the DxG table, the therapies DHA-PPQ, ASAQ, and AL have 97%, 96%, and 92% efficacies, respectively, on wild-type uncomplicated *P. falciparum* cases. Note that AL efficacy studies conducted between 2005 and 2015 were largely done when the 76T allele was circulating at high frequencies, i.e., these were not AL efficacy studies on wild-type falciparum cases. Efficacy of AL on the 76T 86Y Y184 genotype is set to 96% in the model, while efficacy of AL on the K76 N86 184F genotype is set to 89%, assuming wild-type *pfkelch13* and no gene amplification.

Treatment failure due to circulating kelch13 mutants has not yet been observed in Africa, and the effects of *pfkelch13* mutations on treatment failure are believed to be either small or difficult to measure[68,69]. There is much uncertainty in these assessments as epistasis is likely to influence the phenotype of a parasite carrying multiple resistance mutations. As an example, Witkowski et al.'s analysis[26] of 725 patients treated with DHA-PPQ showed that addition of the *pfkelch13* 580Y allele to single-copy plasmepsin parasites increased the treatment failure rate by 1%, but addition of the 580Y allele to multicopy plasmepsin parasites increased the failure rate by 20%. In the present analysis, a single kelch mutation lowers the 28-day efficacy of an ACT by 5–7 percentage points for AL, 3–17% for ASAQ, and 4–35% for DHA-PPQ (ignoring *pfmdr1* amplification, where there is still uncertainty as to its effects[70–72]).

Certain key *P. falciparum* loci have pleiotropic effects on drug resistance. The 76T and 86Y alleles confer some degree of amodiaquine resistance, but the K76 and N86 wild-type alleles confer some level of higher lumefantrine tolerance (or resistance) when compared to their mutant counterparts. At the *pfmdr1* 184 locus, the wild-type Y184 allele is believed to be selected for by amodiaquine, while the derived 184F locus is believed to be selected for by lumefantrine. Copy number of *pfmdr1* gene is known to have effects conferring mefloquine resistance, but the data are conflicting as to whether CNV at this locus confers some level of lumefantrine resistance[70–72]; in the present model and DxG table, an extra copy of *pfmdr1* corresponds to a 5–6% drop in the efficacy of AL, assuming wild-type kelch13.

In this version of the model, patients who fail treatment do not receive re-treatment; these individuals progress to an asymptomatic infection, and their parasites are cleared naturally in 2–8 months if no other treatment is given. One percent of asymptomatic individuals experience a rise in parasitaemia, which becomes symptomatic; these individuals are treated with antimalarials according to the model's standard drug coverage and drug choice parameters.

As in previous publications[11,29,30,49], fitness costs of resistant parasites are set to a 0.0005 daily cost (modeled via slower within-host replication) per resistance locus with an assumption of multiplicative non-epistatic fitness effects. This translates to a 17% per year fitness cost for a genotype carrying a single genetic resistance mechanism.

The mutation rate is set to a 0.001983 per-treatment probability of mutation from a drug-sensitive allele to a drug-resistant allele, in the presence of drug treatment. This "mutation" probability really reflects the combined process of mutation and within-host fixation of the new mutant, as these two events cannot be observed separately. The set value of 0.001983 was calibrated so that the median time from first mutation to 0.01 *pfkelch13* mutant frequency was 7.0 years exactly, in a population of 100,000 individuals with 40% treatment coverage of DHA-PPQ[49]. This 7-year target time was selected based on a probable 5–10 year window from the first occurrence of the 580Y allele in western Cambodia (1980s) to its reaching 0.01 allele frequency (1990s); the earliest data point on 580Y allele frequency is ~0.40 frequency in 2001–2002 in western Cambodia[73].

Treatment strategies

Calibrated model runs were burned in for 10 years to achieve equilibrium (2004–2014) and then run under the treatment coverage settings in Supplementary Table S1 (for another 10 years, 2014–2025), with 43.0% of patients receiving AL in the public sector, 41.2% receiving AL in the private sector, and the remainder receiving sulfadoxine-pyrimethamine (2.1%), chloroquine (1.9%), artesunate monotherapy (4.8%), quinine (0.8%), or amodiaquine monotherapy (6.2%). The post-burn-in calibration period of the model was run until July 1 2025. On July 1, 2025, the model either (1) continued to be run under primarily AL use as a status quo simulation of using AL as first-line therapy for uncomplicated falciparum malaria, or (2) was run under an alternate treatment strategy implemented in the public sector only. Model runs completed on January 1, 2032, and comparisons between treatment strategies and the status quo were done over the 6-year period from July 1, 2025, to July 1, 2031.

Two of the evaluated treatment strategies were first-line therapy switches to either ASAQ or DHA-PPQ. Cycling strategies were evaluated with pre-planned rotation schedules. All possible cycling approaches with two or three ACTs and with 1-year/2-year/3-year rotation periods were considered, for a total of 30 strategies. MFT strategies were implemented as multiple therapies deployed in the same 5 km-by-5 km pixel, with the model using a simple random draw—e.g., under status quo, patients were given AL with 84.2% probability, artesunate monotherapy with 4.8% probability, etc.—to assign a therapy to a particular patient with symptomatic confirmed malaria. All MFT strategies with 50/50 and 75/25 use percentages of two ACTs were considered, along with a 33/33/33 strategy where all three ACTs were used in equal proportion (a total of ten strategies). Ten strategies were run with the triple ACT ALAQ. These strategies included immediate deployment, deployment delayed by four years, and deployment delayed by four years with an interim cycling strategy used before ALAQ deployment. A total of $N = 32$ simulation runs were performed for each strategy, for computational convenience, as 32 was the number of usable cores per node in our computing cluster. Simulation outputs were written into a local SQLite database. No simulation

outputs were excluded. No geographically stratified approaches were considered in this analysis. Supplementary Table S2 shows treatment failure counts for all strategies.

Reporting summary

Further information on research design is available in the Nature Portfolio Reporting Summary linked to this article.

Data availability

All relevant data (simulation outputs) can be found in the GitHub repository: https://github.com/bonilab/Uganda-phase-1—with output files and results stored here https://github.com/bonilab/Uganda-phase-1/releases/tag/v1.0_250505 and a readme file available here https://github.com/bonilab/Uganda-phase-1/blob/main/README.md.

Code availability

All relevant code can be found in the GitHub repository: https://github.com/bonilab/Uganda-phase-1—with a readme file available here https://github.com/bonilab/Uganda-phase-1/blob/main/README.md.

References

1. World Health Organization. *World Malaria Report 2025*, https://www.who.int/teams/global-malaria-programme/reports/world-malaria-report-2025.
2. World Health Organization. *Artemisinin Resistance and Artemisinin-Based Combination Therapy Efficacy: Status Report*, https://iris.who.int/handle/10665/274362 (2018).
3. van Wyk, S. et al. The MARC SE-Africa dashboard: joining forces to counteract emerging antimalarial resistance in South and East Africa. *PLoS Digit. Health* https://doi.org/10.1101/2025.01.07.25320158 (2025).
4. Rosenthal, P. J., Asua, V. & Conrad, M. D. Emergence, transmission dynamics and mechanisms of artemisinin partial resistance in malaria parasites in Africa. *Nat. Rev. Microbiol.* **22**, 373–384 (2024).
5. Akala, H. et al. Detection of twenty-four *Plasmodium Falciparum* Kelch13 mutations including C469Y, P553L, R561H, and A675V across Kenya. *SSRN*, https://doi.org/10.2139/ssrn.5020665 (2024).
6. Dhorda, M. et al. Artemisinin-resistant malaria in Africa demands urgent action. *Science* **385**, 252–254 (2024).
7. Ishengoma, D. S. et al. Urgent action is needed to confront artemisinin partial resistance in African malaria parasites. *Nat. Med.* **30**, 1807–1808 (2024).
8. Rosenthal, P. J. et al. The emergence of artemisinin partial resistance in Africa: how do we respond? *Lancet Infect. Dis.* **24**, e591–e600 (2024).
9. World Health Organization. *Multiple First-Line Therapies as Part of the Response to Antimalarial Drug Resistance: An Implementation Guide*, https://who.int/publications/i/item/9789240103603 (2024).
10. World Health Organization. *Strategy to Respond to Antimalarial Drug Resistance in Africa* (WHO, 2022).
11. Zupko, R. J. et al. Modeling policy interventions for slowing the spread of artemisinin-resistant pfkelch R561H mutations in Rwanda. *Nat. Med.* **29**, 2775–2784 (2023).
12. Boni, M. F., White, N. J. & Baird, J. K. The community as the patient in malaria-endemic areas: preempting drug resistance with multiple first-line therapies. *PLoS Med.* **13**, e1001984 (2016).
13. Boni, M. F., Soulama, I., Opigo, J., Watson, O. J. & Ogutu, B. Slowing artemisinin resistance in Africa. *Sci. Adv.* **11**, eaeb7618 (2025).
14. Okitwi, M. et al. Changes in susceptibility of *Plasmodium falciparum* to antimalarial drugs in Uganda over time: 2019-2024. *Nat. Commun.* **16**, 7353 (2025).
15. Niaré, K. et al. A novel locus associated with decreased susceptibility of *Plasmodium falciparum* to lumefantrine and dihydroartemisinin has emerged and spread in Uganda. Preprint at https://doi.org/10.1101/2025.07.30.667738 (2025).
16. Kamya, M. R. et al. Efficacies of artemether–lumefantrine, artesunate–amodiaquine, dihydroartemisinin–piperaquine, and artesunate–pyronaridine for the treatment of uncomplicated *Plasmodium falciparum* malaria in children aged 6 months to 10 years in Uganda: a randomised, open-label, phase 4 clinical trial. *Lancet Infect. Dis.* **26**, 67–78 (2026).
17. Gansané, A. et al. Anti-malarial efficacy and resistance monitoring of artemether-lumefantrine and dihydroartemisinin-piperaquine shows inadequate efficacy in children in Burkina Faso, 2017–2018. *Malar. J.* **20**, 48 (2021).
18. Rueangweerayut, R. et al. Pyronaridine–artesunate versus mefloquine plus artesunate for malaria. *New Engl. J. Med.* **366**, 1298–1309 (2012).
19. Pryce, J., Taylor, M., Fox, T. & Hine, P. Pyronaridine-artesunate for treating uncomplicated *Plasmodium falciparum* malaria. *Cochrane Database Syst. Rev.* **2022**, CD006404 (2022).
20. Alebachew, M. et al. Therapeutic efficacy of pyronaridine-artesunate (Pyramax®) against uncomplicated *Plasmodium falciparum* infection at Hamusit Health Centre, Northwest Ethiopia. *Malar. J.* **22**, 186 (2023).
21. Falade, C. O. et al. Efficacy and safety of pyronaridine–artesunate versus artemether–lumefantrine in the treatment of acute uncomplicated malaria in children in South-West Nigeria: an open-labelled randomized controlled trial. *Malar. J.* **22**, 154 (2023).
22. Dimbu, P. R. et al. Therapeutic response to four artemisinin-based combination therapies in Angola, 2021. *Antimicrob. Agents Chemother.* **68**, e01525–23 (2024).
23. Conrad, M. D. et al. Evolution of partial resistance to artemisinins in malaria parasites in Uganda. *New Engl. J. Med.* **389**, 722–732 (2023).
24. World Health Organization. *World Malaria Report 2024*, https://www.who.int/teams/global-malaria-programme/reports/world-malaria-report-2024.
25. USAID. DHS Program, Spatial Data Repository—Boundaries, https://spatialdata.dhsprogram.com/boundaries/#countryId=UG&view=table (2024).
26. Witkowski, B. et al. A surrogate marker of piperaquine-resistant *Plasmodium falciparum* malaria: a phenotype–genotype association study. *Lancet Infect. Dis.* **17**, 174–183 (2017).
27. Uganda Ministry of Health. *Strategy to Respond to Antimalarial Drug Resistance in Uganda* (Uganda Ministry of Health, 2025).
28. Boni, M. F., Smith, D. L. & Laxminarayan, R. Benefits of using multiple first-line therapies against malaria. *Proc. Natl. Acad. Sci. USA* **105**, 14216–14221 (2008).
29. Zupko, R. J. et al. Long-term effects of increased adoption of artemisinin combination therapies in Burkina Faso. *PLoS Glob. Public Health* **2**, e0000111 (2022).
30. Nguyen, T. D. et al. Preventing antimalarial drug resistance with triple artemisinin-based combination therapies. *Nat. Commun.* **14**, 4568 (2023).
31. Tran, K. T. et al. Effects of recombination on multi-drug resistance evolution in *Plasmodium falciparum* malaria. *PLoS Comput. Biol.* **21**, e1013401 (2025).
32. Rehwagen, C. WHO ultimatum on artemisinin monotherapy is showing results. *BMJ* **332**, 1176 (2006).
33. Giao, P. T. et al. Artemisinin for treatment of uncomplicated falciparum malaria: is there a place for monotherapy? *Am. J. Trop. Med. Hyg.* **65**, 690–695 (2001).
34. International Artemisinin Study Group Artesunate combinations for treatment of malaria: meta-analysis. *Lancet* **363**, 9–17 (2004).
35. White, N. J. Antimalarial drug resistance. *J. Clin. Investig.* **113**, 1084–1092 (2004).

36. World Health Organization. *Guidelines for the Treatment of Malaria, First Edition*, https://ec.europa.eu/echo/files/policies/sectoral/health_2006_malaria_treatment_guidelines_who.pdf (2006).
37. Osoro, C. B. et al. Perceptions and drivers of healthcare provider and drug dispenser practices for the treatment of malaria in pregnancy in the context of multiple first-line therapies in western Kenya: a qualitative study. *Malar. J.* **22**, 274 (2023).
38. Gindola, Y. et al. Adherence to national malaria clinical management and testing guidelines in selected private clinics of Gambela Town, Gambela Region, Ethiopia: a mixed method study. *Malar. J.* **21**, 164 (2022).
39. Wang, L. T. et al. Private sector drug shops frequently dispense parenteral anti-malarials in a rural region of Western Uganda. *Malar. J.* **17**, 305 (2018).
40. Uganda Ministry of Health National Malaria Control Division. *Uganda Malaria Indicator Survey 2018–2019*, https://dhsprogram.com/pubs/pdf/MIS34/MIS34.pdf (2020).
41. Mavoko, H. M. et al. Efficacy and safety of re-treatment with the same artemisinin-based combination treatment (ACT) compared with an alternative ACT and quinine plus clindamycin after failure of first-line recommended ACT (QUINACT): a bicentre, open-label, phase 3, randomised controlled trial. *Lancet Glob. Health* **5**, e60–e68 (2017).
42. Ebong, C. et al. Efficacy and safety of artemether-lumefantrine and dihydroartemisinin-piperaquine for the treatment of uncomplicated *Plasmodium falciparum* malaria and prevalence of molecular markers associated with artemisinin and partner drug resistance in Uganda. *Malar. J.* **20**, 484 (2021).
43. Agaba, B. B. et al. Emerging threat of artemisinin partial resistance markers (pfk13 mutations) in *Plasmodium falciparum* parasite populations in multiple geographical locations in high transmission regions of Uganda. *Malar. J.* **23**, 330 (2024).
44. Mullard, A. Novel antimalarial passes key phase III test. *Nat. Rev. Drug Discov.* **25**, 8–8 (2025).
45. Ogutu, B. et al. Ganaplacide (KAF156) plus lumefantrine solid dispersion formulation combination for uncomplicated *Plasmodium falciparum* malaria: an open-label, multicentre, parallel-group, randomised, controlled, phase 2 trial. *Lancet Infect. Dis.* **23**, 1051–1061 (2023).
46. Stepniewska, K. et al. Efficacy of single-dose primaquine with artemisinin combination therapy on *Plasmodium falciparum* gametocytes and transmission: an individual patient meta-analysis. *J. Infect. Dis.* **225**, 1215–1226 (2022).
47. Yilma, D. et al. Safety and efficacy of single-dose primaquine to interrupt *Plasmodium falciparum* malaria transmission in children compared with adults: a systematic review and individual patient data meta-analysis. *Lancet Infect. Dis.* **25**, 965–976 (2025).
48. Nguyen, T. D., Tran, T. N.-A., Parker, D. M., White, N. J. & Boni, M. F. Antimalarial mass drug administration in large populations and the evolution of drug resistance. *PLoS Glob. Public Health* **3**, e0002200 (2023).
49. Watson, O. J. et al. Pre-existing partner-drug resistance facilitates the emergence and spread of artemisinin resistance: a consensus modelling study. *Lancet Microbe* **3**, 701–710 (2022).
50. van der Pluijm, R. W. et al. Determinants of dihydroartemisinin-piperaquine treatment failure in *Plasmodium falciparum* malaria in Cambodia, Thailand, and Vietnam: a prospective clinical, pharmacological, and genetic study. *Lancet Infect. Dis.* **19**, 952–961 (2019).
51. Mok, S. et al. Mapping the genomic landscape of multidrug resistance in *Plasmodium falciparum* and its impact on parasite fitness. *Sci. Adv.* **9**, eadi2364 (2023).
52. Small-Saunders, J. L. et al. Evidence for the early emergence of piperaquine-resistant *Plasmodium falciparum* malaria and modeling strategies to mitigate resistance. *PLOS Pathog.* **18**, e1010278 (2022).
53. Ross, L. S. et al. Emerging Southeast Asian PfCRT mutations confer *Plasmodium falciparum* resistance to the first-line antimalarial piperaquine. *Nat. Commun.* **9**, 3314 (2018).
54. Dhingra, S. K., Small-Saunders, J. L., Ménard, D. & Fidock, D. A. *Plasmodium falciparum* resistance to piperaquine driven by pfCRT. *Lancet Infect. Dis.* **19**, 1168–1169 (2019).
55. Kaboré, J. M. T. et al. Feasibility and acceptability of a strategy deploying multiple first-line artemisinin-based combination therapies for uncomplicated malaria in the health district of Kaya, Burkina Faso. *Trop. Med. Infect. Dis.* **8**, 195 (2023).
56. Hien, D. et al. Stakeholder perceptions on the deployment of multiple first-line therapies for uncomplicated malaria: a qualitative study in the health district of Kaya, Burkina Faso. *Malar. J.* **21**, 202 (2022).
57. Cole, A. et al. Health system challenges and facilitators associated with adaptive cycling deployment of multiple first-line treatment for uncomplicated malaria: a pilot study in a malaria-endemic region of Kenya. *Malar. J.* **24**, 328 (2025).
58. Nuwa, A. et al. Effectiveness of sulfadoxine–pyrimethamine plus amodiaquine and dihydroartemisinin–piperaquine for seasonal malaria chemoprevention in Uganda: a three-arm, open-label, non-inferiority and superiority, cluster-randomised, controlled trial. *Lancet Infect. Dis.* **25**, 726–P736 (2025).
59. Tukwasibwe, S. et al. Varied prevalence of antimalarial drug resistance markers in different populations of newly arrived refugees in Uganda. *J. Infect. Dis.* **230**, 497–504 (2024).
60. Symons, T. L. et al. Estimating the potential malaria morbidity and mortality avertable by the US President's Malaria Initiative in 2025: a geospatial modelling analysis. *Lancet* **405**, 2231–2240 (2025).
61. Winskill, P. et al. Rapid response modelled estimates of the effect of the US global aid freeze on President's Malaria Initiative impact in sub-Saharan Africa. Preprint at https://spiral.imperial.ac.uk/entities/publication/9dc45650-271d-4fdb-8f1a-baabdb019c85 (2025).
62. Humanitarian Data Exchange. Uganda—Subnational Administrative Boundaries— Humanitarian Data Exchange, https://data.humdata.org/dataset/cod-ab-uga.
63. WorldPop. Global 100m population total adjusted to match the corresponding UNPD estimate, https://doi.org/10.5258/SOTON/WP00660 (University of Southampton, 2020).
64. Weiss, D. J. et al. A global map of travel time to cities to assess inequalities in accessibility in 2015. *Nature* **553**, 333–336 (2018).
65. Wesolowski, A., O'Meara, W. P., Eagle, N., Tatem, A. J. & Buckee, C. O. Evaluating spatial interaction models for regional mobility in sub-Saharan Africa. *PLoS Comput. Biol.* **11**, e1004267 (2015).
66. Zupko, R. J., Nguyen, T. D., Wesolowski, A., Gerardin, J. & Boni, M. F. National-scale simulation of human movement in a spatially coupled individual-based model of malaria in Burkina Faso. *Nat. Sci. Rep.* **13**, 321 (2023).
67. Amaratunga, C. et al. Association of mutations in the *Plasmodium falciparum* Kelch13 gene (Pf3D7_1343700) with parasite clearance rates after artemisinin-based treatments—a WWARN individual patient data meta-analysis. *BMC Med.* **17**, 1 (2019).
68. Mihreteab, S. et al. Increasing prevalence of artemisinin-resistant HRP2-negative malaria in Eritrea. *New Engl. J. Med.* **389**, 1191–1202 (2023).
69. Uwimana, A. et al. Association of *Plasmodium falciparum* kelch13 R561H genotypes with delayed parasite clearance in Rwanda: an open-label, single-arm, multicentre, therapeutic efficacy study. *Lancet Infect. Dis.* **21**, 1120–1128 (2021).
70. Venkatesan, M. et al. Polymorphisms in *Plasmodium falciparum* chloroquine resistance transporter and multidrug resistance 1 genes: parasite risk factors that affect treatment outcomes for *P. falciparum* malaria after artemether-lumefantrine and artesunate-amodiaquine. *Am. J. Trop. Med. Hyg.* **91**, 833–843 (2014).

71. Venkatesan, M. Erratum: polymorphisms in *Plasmodium falciparum* chloroquine resistance transporter and multidrug resistance 1 genes. *Am. J. Trop. Med. Hyg.* **100**, 766 (2019).
72. Fançony, C. et al. Artemether-lumefantrine treatment selects *Plasmodium falciparum* multidrug resistance 1 (pfmdr1) increased copy number among African malaria infections. *J. Infect. Dis.* **231**, e1119–e1128 (2025).
73. Ariey, F. et al. A molecular marker of artemisinin-resistant *Plasmodium falciparum* malaria. *Nature* **505**, 50–55 (2014).

Acknowledgements

This article is dedicated to the memory and legacy of Professor Nicholas J White. Computations for this research were performed on the Pennsylvania State University's Institute for Computational and Data Sciences' Roar supercomputer and on Temple University's College of Science and Technology Owl's Nest Cluster.

Author contributions

Conceptualization: M.F.B., J.O., B.B.A., M.R.K., and G.B.R. Formal analysis: T.D.N., R.J.Z. Funding acquisition: M.F.B. Investigation: T.D.N., R.J.Z., M.D.C., C.C.F., V.A., K.T.T., and D.M.G. Methodology: T.D.N., R.J.Z., M.D.C., C.C.F., V.A., K.T.T., and D.M.G. Supporting data: M.D.C., P.J.R., G.B.R., B.B.A., M.R.K., and J.O. Software: T.D.N., R.J.Z., and K.T.T. Supervision: M.F.B., J.O. Visualization: T.D.N., R.J.Z., and C.C.F. Writing–original draft: M.F.B. Writing–review & editing: M.F.B., T.D.N., P.J.R., and M.D.C.

Funding

T.D.N., R.J.Z., K.T.T., C.C.F., M.F.B., and D.M.G. were funded by National Institutes of Health grant NIAID R01AI153355 and Bill and Melinda Gates Foundation grant INV-005517. T.D.N., K.T.T., C.C.F., and M.F.B. were funded by National Institutes of Health grant NIAID R01AI153355 and Bill and Melinda Gates Foundation grant INV-056612. V.A. was funded by a Bill and Melinda Gates Foundation grant INV-037316. G.B.R., B.B.A., M.R.K., and J.O. are funded by the US President's Malaria Initiative prime contract 72061722C00003 and sub-contract 14070-IDRC-01. The study was additionally funded by the National Institutes of Health (R01AI075045, R01AI173557, U19AI089674, RO1AI117001, R01AI139179, and D43TW010526), the Medicines for Malaria Venture (RD/15/0001), and the Gates Foundation (INV-035751).

Competing interests

P.J.R. consulted for GSK in 2023 and Merck in 2024 on new antimalarial drug discovery. No other authors have any competing interests.

Additional information

Supplementary information The online version contains Supplementary material available at https://doi.org/10.1038/s41467-026-74737-y.

Correspondence and requests for materials should be addressed to Maciej F. Boni.

Peer review information *Nature Communications* thanks the anonymous reviewers for their contribution to the peer review of this work. A peer review file is available.